STREAM DEPLETION AND PUMPING TEST INTERPRETATION

IN A HORIZONTALLY ANISOTROPIC AQUIFER NEAR A

STREAM

A Thesis

by

YIBIN HUANG

Submitted to the Office of Graduate and Professional Studies of
Texas A&M University
in partial fulfillment of the requirements for the degree of

MASTER OF SCIENCE

Chair of Committee: Hongbin Zhan
Committee Members: Peter Knappett
                                  David Sparks
Head of Department: Ronald Kaiser

December 2016

Major Subject: Water Management and Hydrological Science

ABSTRACT

Conventional pumping test theories such as Theis solution often assume a horizontally isotropic media. Horizontal anisotropy exists in certain aquifer settings and its impact on pumping tests is not clearly demonstrated before, particularly when the aquifer is bounded by a stream. In this thesis, based on a newly developed mathematical model for pumping tests in a horizontally anisotropic aquifer bounded by a stream, the corresponding interpretation procedures will be illustrated. Stream depletion will be calculated as a result of stream bank pumping based on the new model as well. The results of this research reflect that (1) aquifer parameters derived from newly developed interpretation methods are acceptable in the range of allowable error; so these methods can be used in practical field experiment; (2) with the increase of T_α/T_β, stream depletion rate under the steady state also increases where T_α and T_α are the major and minor principal transmissivity values ($T_\alpha > T_\beta$); (3) when the angle between the *X* axis and the direction of T_α increases from 0 to $\frac{\pi}{2}$, stream depletion increases, where the *X*-axis is one of the working coordinate; conversely, when such an angle increases from $\frac{\pi}{2}$ to π, stream depletion decreases. This research is expected to fill the gap of knowledge on present stream-aquifer interaction and pumping test theories for aquifers.

ACKNOWLEDGMENTS

It would not be possible to finish this master thesis without the help and support of so many kind people around me.

Firstly, I would like to express my gratitude to my advisor Dr. Hongbin Zhan. He was very patient to answer all my questions whatever it is about my research or writing. He also helped me revise my thesis over and over again. Thanks for his guidance during the entire process.

Secondly, I appreciate Drs. Peter Knappett and David Sparks for giving me many useful advices about my thesis. Their advices helped me improve my research and thesis.

Finally, I am grateful that so many amazing friends helped me from all aspects and would like to thank my friends for their support. Such as, my roommate Yue Sun; my officemates Xin Liu and Zhe Cao; my friends Chen Ling and Wang Xiang.

NOMENCLATURE

Q	Constant pumping rate, (m^3/s)
s	Drawdown induced by pumping, (m)
S	Storativity of confined aquifer or specific yield of unconfined aquifer, (dimensionless)
t	Time from the beginning of pumping, (s)
T	Transmissivity, T with subscript represents the component of transmissivity on that direction, (m^2/s)
L	Stream length, (m)
q	Water flux through unit stream length per unit time, subscript means the direction of it, (m^2/s)
Q_D	Stream depletion rate along the stream during the pumping test, (m^3/s)
T_e	Equivalent scalar transmissivity, (m^2/s)
J	Hydraulic gradient, subscript represents the direction of the gradient, (dimensionless)
X and Y	Orthogonal horizontal axes of working coordinate system, (m)
α and β	Orthogonal horizontal axes of principal coordinate system, (m)
α^* and β^*	Orthogonal horizontal axis in equivalent isotropic domain,

	(m)
α_1 and β_1	The coordinates of observation well in $\alpha\beta$ system, (m)
α_1^* and β_1^*	The coordinates of observation well in $\alpha^*\beta^*$ system, (m)
θ, η, ξ and γ	Degree of angle, (dimensionless)
a and b	The intercepts of stream on α and β axis, separately, (m)
$a^{'}$ and $b^{'}$	The intercepts of stream on α^* and β^* axis, separately, (m)
X_0	Shortest distance between the pumping well and the stream, (m)
X_1 and Y_1	The coordinate of the first observation well in the XY system, (m)
l	The shortest distance between pumping well and stream in $\alpha^*\beta^*$ system, (m)
R_1 and R_2	The equivalent distance between observation well and pumping well, image well in XY system, (m)
r_1, r_2 and r_3	The straight-line distance between pumping well and three observation wells, separately, (m)
D	Hydraulic diffusivity, subscript means the different observation wells, (m^2/s)
s_i	Drawdown at the inflection point, (m)
t_i	Pumping time at the inflection point, (s)

CONTRIBUTORS AND FUNDING SOURCES

Contributors

This work was supervised by the thesis committee consisting of Dr. Hongbin Zhan,

Dr. Peter Knappett and Dr. David Sparks of the Department of Geology and Geophysics.

All work for this thesis was completely conducted by the student.

Funding Sources

TABLE OF CONTENTS

LIST OF FIGURES

LIST OF TABLES

1. INTRODUCTION

Groundwater is one of the most important natural resources, which occupies 30% of freshwater in the world (Herschy and Fairbridge, 1998). Although groundwater is buried beneath ground surface, in many cases, it is not isolated and has interactions with surface water, like streams, lakes and wetlands (Winter, 1998). Ground-surface water interaction is an important component of hydrological budgets and has significant effect on socioeconomic and geopolitical aspects (Butler et al., 2001). Because of concerns about acid rain, stream restoration, groundwater over-exploitation and other various environmental and social problems, the interactions between groundwater and stream attract great attention. Groundwater and stream interaction can primarily proceed in two ways, one is groundwater recharges stream through the streambed (the so-called base flow) when the hydraulic head of groundwater is greater than surface water; the other is stream water infiltrates the groundwater through the streambed when the stream stage has a higher head than the adjacent aquifer (Sophocleous, 2002, Kalbus et al., 2006). In some watersheds, groundwater can provide 50%-80% of annual stream flow, which could carry significant amount of nutrient to aquatic animals and plants at the same time (Hill, 1990). With the increase of water demand, the natural process of groundwater-stream interactions is artificially disturbed by pumping groundwater near the stream. Hantush (1959) introduced several purposes of well installation near a stream. One of them is inducing

infiltration from streams to underlying materials. Another is artificially decreasing natural flow that have been discharged to the streams.

When a pumping well is installed near a stream and starts pumping, aquifer storage initially provides water to the pumping well and a cone of depression is created near the well. With the increase of pumping time, the cone of depression extends gradually and intercepts stream eventually. If the stream is hydraulically connected with the surrounding aquifer without any barriers, the stream may be considered as a constant-head boundary (CHB). When the hydraulic head at the aquifer adjacent to a stream is lower than the stream stage, water will flow away from the stream to the aquifer, which is called stream depletion. Jenkins (1968) gave an explicit definition of stream depletion as either direct depletion from the stream or reduction of return flow to the stream. Compared with natural conditions, a direct influence of stream depletion is the decrease of stream flow amount, which will cause negative impacts on aquatic ecosystems, availability of surface water, quality and aesthetic value of streams and other water-resource management issues (Barlow and Leake, 2012).

In the United States, stream depletion is a serious problem in many states. For instance, the Platte River, a tributary of Missouri River, is a major river in Nebraska and flows from west to east through the state, which is hydrologically connected with surrounding aquifers. Chen (2007) stated that because of tremendous groundwater exploitation for irrigation usage, stream depletion caused serious water issues in the Platte River valley. On the one hand, groundwater pumping reduced the stream flow greatly. On the other hand, non-point contamination threatened the quality of stream water. Both factors harmed the health of

stream and the ecosystem of the Platte River valley. A similar problem also appeared in Kansas in the past decades. The reduction of stream flow as the result of groundwater decline significantly impacted the fish and wildlife resources in and along the Arkansas River and other streams in western and south-central Kansas (Sophocleous et at., 1988). The situation promoted the establishment of minimum desirable stream flow standards in Kansas in the early 1980s by Kansas Legislature (Sophocleous et at., 1995). Besides the United States, regions in South America, North Africa, Middle East, Southern Europe, East and Southeast Asia also have severe stream depletion problems (Foglia et al., 2013).

Numerous studies have made significant contributions to understand the processes and factors that affect stream depletion by pumping wells over the past few decades. Moreover, the methods used to estimate stream depletion rate and amount have also been well developed. For example, Theis (1941) and Glover and Balmer (1954) derived fundamental equations calculating the stream depletion rate at any location of the stream and the total depletion of the whole river during a given period. A main technique used in their work is image-well method, i.e., an image recharge well that has the same rate as the pumping well is added on the other side of the river, which is symmetric with the pumping well in respect to the stream. Such an image recharge well serves the same role as the stream hydraulically. The drawdown at any location of the study area will be the superposition of drawdowns (or buildup) generated by both the (original) pumping well and the (image) recharge well. Based on the work of Theis (1941) and Glover and Balmer (1954), some advanced works have also been developed. For instance, Jenkins (1968) stressed the residual effect on stream depletion after the cessation of pumping, if groundwater can only

be recharged by an intercepted stream. Butler et al. (2001) focused on stream depletion problems for a stream that partially penetrates the aquifer. Butler et al. (2007) and Hunt (2009) interested on stream depletion in leaky aquifers. Yeh et al. (2008) focused on stream depletion in wedge-shaped aquifer. Tsou et al. (2010) discussed stream depletion caused by horizontal or slanted wells in confined aquifers. While, in some cases, observed pumping test data already reflect the existence of stream depletion, but the location of the hidden streams or underground streams such as karst channels is unknown. Sageev et al. (1985), Chapuis (1994) and Singh (2002) used different methods to analyze the observed pumping test data, which were subsequently used to detect the location of such hidden recharge boundary.

Besides stream depletion issues, hydrogeologists are also interested in determining aquifer properties such as transmissivity, storativity based on pumping test data. When a pumping well is located near a stream, the drawdown curve is certainly different from that without a stream. Hantush (1959) developed several graphic methods for determining the hydraulic parameters of aquifer laterally bounded by one recharge boundary. Singh (2002) suggested a method that required a much shorter pumping duration for identifying aquifer parameters.

For all of aforementioned works, the aquifer is assumed to be homogeneous and horizontally isotropic. Different controlling factors, such as sediment deposition rate, deposition environment, shape and orientation of sediment particles and others all can preclude the formation of a horizontally isotropic aquifer (Quinones-Aponte, 1989). This indicates that more realistic and accurate model of groundwater flow needs to consider the

horizontally anisotropy of the aquifer (Quiñones-Aponte, 1989). Papadopulos (1965) and Hantush (1966) stated that at least four wells were needed to determine aquifer parameters in a horizontally anisotropic aquifer: one pumping well and three non-collinear observation wells. Neuman et al. (1984) proposed a new pumping test scheme in which only three wells were needed to analyze data.

Vertical anisotropy is very common in the field, such as alluvial aquifer because of the process of sedimentation. In general, horizontal hydraulic conductivity is often one to two orders of magnitude larger than the vertical one, and such a vertical anisotropy can play an important role in controlling stream-aquifer interactions, particularly when vertical flow is of concern near the stream (Chen and Yin, 1999). Stream depletion in vertically anisotropic aquifers have been extensively investigated over many decades (Chen, 2000; Chen and Chen, 2003; Cheng et al., 2011).

After extensive literature review, there is little research related to pumping near a stream concerning the horizontal aquifer anisotropy. Different from vertical anisotropy, when a horizontally anisotropic aquifer is pumped, equipotential lines are elliptical rather than circular in a planar view. Horizontal anisotropy may be developed in several geological settings. For example, Stoner (1981) introduced that thick coal beds exhibit a systematic set of fractures that almost perpendicular to bedding, which result in significantly horizontal anisotropy in Sawyer-A and Anderson coal aquifers, Montana. As part of U.S. Geological Survey program known as "Caribbean Islands Regional Aquifer-System Analysis", Quiñones-Aponte (1989) performed an aquifer test in Salinas alluvial fan in the southern part of Puerto Rico. By analyzing collected test data, it indicated that

in the study area, the major and minor transmissivity tensor are 3,608 and 2,228 m^2/day, respectively, and the ratio of horizontal anisotropy in the area varies from 1.62 to 1.00. Recently, Cook and Barlas (2014) launched four pumping test in the Pen Argyl Member of the Martinsburg Formation in Pennsylvania, and used statistical tests to determine the direction and magnitude of principal transmissivity. The results showed that major and minor transmissivity are 582 m^2/day and 65 m^2/day, separately, and the counter-clockwise angle between the direction of major transmissivity and X axis is $41.5° \pm 8.8°$. There are also many publications addressing groundwater flow in horizontally anisotropic aquifers (Lebbe and Breuck, 1997; Mathias and Butler, 2007; Wen et al., 2010; Cihan et al., 2014).

The aim of this thesis is developing a new mathematical model to process pumping test data near a stream in a horizontally anisotropic aquifer. I will propose a new procedure to determine aquifer properties for such a situation, and propose new equations to calculate stream depletion with specific consideration of horizontal anisotropy. This research fills the gap of pumping induced groundwater-surface water interaction in horizontally anisotropic aquifers.

2. PROBLEM STATEMENT

2.1 Conceptual Model

To simplify the problem, the stream is assumed to be a CHB, which is a straight line and fully penetrates the entire aquifer (Singh, 2002). If a semi-permeable river bed exists, then the river cannot be treated as a CHB and instead is often treated as a general-head boundary (GHB). The discussion of GHB is out of scope of this thesis and will be pursued in a future study. Nevertheless, based on the CHB assumption, the conceptual model of the problem is shown in Figure 1. The aquifer is bounded laterally by a straight stream, the pumping well that has a constant pumping rate is also fully penetrating.

The properties of aquifer are homogeneous and horizontally anisotropic, as shown in Figure 2. X and Y are the orthogonal axes of a working coordinate system and the Y axis is parallel with the stream. α and β are the orthogonal axes of a principal coordinate system. Principal transmissivities are T_α and T_β, and T_α is the major component that satisifies that $T_\alpha > T_\beta$. The pumping well is located at the origin of the working coordinate system and has a constant pumping rate. The shortest distance between the pumping well and the stream is X_0. The stream intercepts α and β axes at (a,0) and (0, -b), respectively. Usually, for a horizontally anisotropic aquifer in the field, the principal direction of transmissivity is unknown. Therefore, it is assumed that the major component of principal transmissivity (T_α) forms an angle θ with the X axis. The value of θ will be determined later.
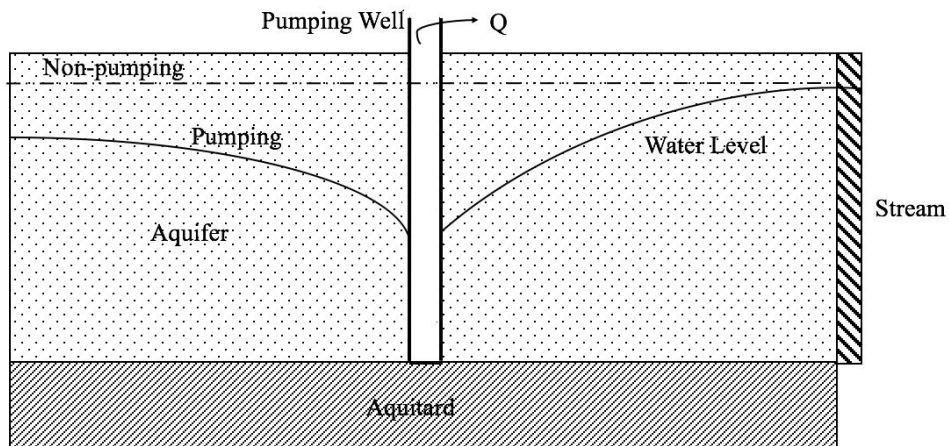
Figure 1： Graphic view of studied aquifer bounded by a stream (After Ferris et al. 1962).
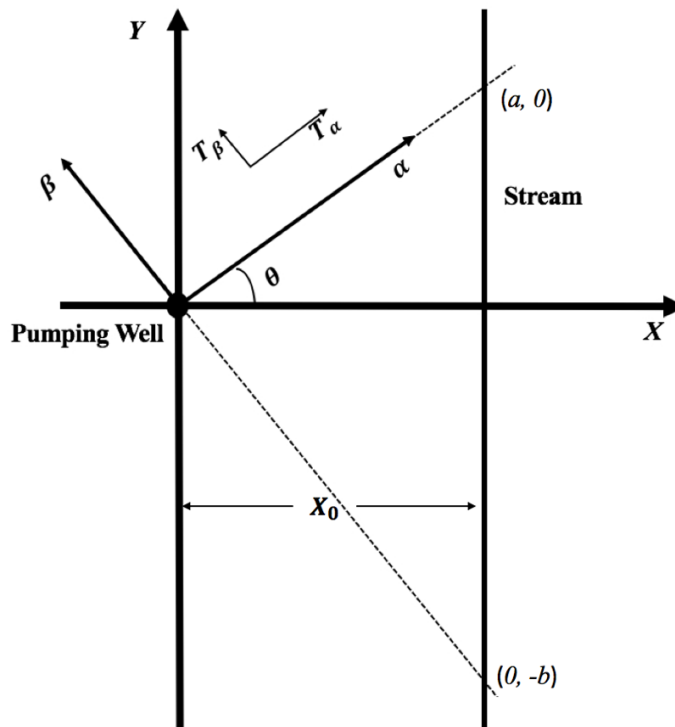

Figure 2: The outline of studied aquifer. α and β are the principal coordinates; X and Y are the working coordinates. The origins of both coordinates are located at the pumping well.

2.2 Main Tasks

I will follow the following procedures to investigate the problem.

Firstly, the drawdown equation is derived as follows. Theis (1941) and Glover and Balmer (1954) established the foundation of solving stream depletion problems, and both studies assumed that the pumped aquifer is horizontally isotropic, which can directly use the following Eqs. (2-1) and (2-2) to describe drawdown distribution.

$$s = \frac{Q}{4\pi T} W(u) = \frac{Q}{4\pi T} \int_u^{+\infty} \frac{e^{-\lambda}}{\lambda} d\lambda \ , \tag{2-1}$$

$$u = \frac{r^2 S}{4Tt} \ , \tag{2-2}$$

where s is drawdown; Q is the pumping rate; r is the radial distance between the pumping well and an arbitrary observation well; t is time since pumping starts; T and S are transmissivity and storativity of an isotropic aquifer, respectively. While the domain of interest in the conceptual model of this thesis is horizontally anisotropic rather than isotropic, thus new drawdown equations rather than above Eqs. (2-1) and (2-2) will be discussed in the following Chapter 3.1.

Secondly, the aquifer properties are determined based on the newly developed drawdown equations as follows. If the aquifer is confined, transmissivity and storativity represent its main properties. If the aquifer is unconfined, a modified procedure based on the procedure used for confined aquifer will be used (discussed in Chapter 3.2). The following questions will be answered in Chapter 3.2: 1) How to design an appropriate pumping test to determine such parameters values in a horizontally anisotropic aquifer? 2) How many minimum observation wells are needed to determine the parameter values in a

horizontally anisotropic aquifer? The detailed steps of pumping test interpretation in a horizontally anisotropic aquifer will be discussed in Chapter 3.2.

Thirdly, the stream depletion rate is determined. In order to evaluate the effect of pumping on the stream flow, depletion rate is an important criterion. This part will be explained in Chapter 3.3.

Fourthly, the effect of the horizontal anisotropy is specifically checked. For a horizontally anisotropic aquifer, its properties are mainly controlled by θ and the ratio of T_α/T_β. Keeping all other parameters constant and changing the values of θ or T_α/T_β conclude its influence on the depletion rate, which will be discussed in Chapter 3.3.

3. METHODOLOGY

The four tasks listed in Chapter 2.2 will be tackled orderly.

3.1 Drawdown Equation

When studying groundwater flow in a horizontally anisotropic aquifer, it is advisable to change the horizontally anisotropic aquifer into an equivalent isotropic aquifer. Neuman et al. (1984) proposed a method to describe drawdown in a horizontally anisotropic aquifer, in which the principal coordinates form an angle θ with the working coordinates XY as shown in Figure 2. By using coordinates transformation, the relationship between two coordinate systems satisfies

$$\begin{cases} \alpha = X\cos\theta + Y\sin\theta \\ \beta = -X\sin\theta + Y\cos\theta \end{cases} . \tag{3-1}$$

For a horizontally anisotropic aquifer, the general form of transmissivity tensors in the working (XY) and principal ($\alpha\beta$) coordinate systems are respectively

$$\overline{\overline{T_{XY}}} = \begin{vmatrix} T_{XX} & T_{XY} \\ T_{YX} & T_{YY} \end{vmatrix}, \quad \overline{\overline{T_{\alpha\beta}}} = \begin{vmatrix} T_\alpha & 0 \\ 0 & T_\beta \end{vmatrix} . \tag{3-2}$$

Because of the existence of non-zero θ values, the off-diagonal terms of the transmissivity tensor satisfy

$$T_{XY} = T_{YX} \neq 0 . \tag{3-3}$$

Therefore, the flow governing equation in the XY system is

$$T_{XX} \frac{\partial^2 s}{\partial X^2} + 2T_{XY} \frac{\partial^2 s}{\partial X \partial Y} + T_{YY} \frac{\partial^2 s}{\partial Y^2} = S \frac{\partial s}{\partial t} . \tag{3-4}$$

While, in the principal coordinate system, the flow is governed by

$$T_\alpha \frac{\partial^2 s}{\partial \alpha^2} + T_\beta \frac{\partial^2 s}{\partial \beta^2} = S \frac{\partial s}{\partial t} \, , \tag{3-5}$$

and the relationship between two sets of transmissivity tensors is (Bear, 1972)

$$\begin{cases} T_{XX} = T_\alpha cos^2\theta + T_\beta sin^2\theta \\ T_{YY} = T_\alpha sin^2\theta + T_\beta cos^2\theta \\ T_{XY} = T_{YX} = (T_\alpha - T_\beta)sin\theta cos\theta \end{cases} . \tag{3-6}$$

In the $\alpha\beta$ coordinate system, the domain of interest is anisotropic, so the corresponding

drawdown equation Eq. (3-5) is still not convenient to use. Thus, it is transformed into an

equivalent isotropic form by defining a new set of coordinates α^* and β^*, which are

parallel to α and β, respectively. One has

$$\alpha^* = \sqrt{\frac{T_\beta}{T_e}}\alpha; \quad \beta^* = \sqrt{\frac{T_\alpha}{T_e}}\beta \, . \tag{3-7}$$

where T_e is the equivalent scalar tansmissivity and the steps about deriving the

expression of T_e are shown in Appendix A,

$$T_e = \sqrt{T_\alpha T_\beta} = \sqrt{T_{XX}T_{YY} - T_{XY}^2} \, . \tag{3-8}$$

Substituting Eq. (3-7) into Eq. (3-5) will result in

$$T_e \left(\frac{\partial^2 s}{\partial \alpha^{*2}} + \frac{\partial^2 s}{\partial \beta^{*2}} \right) = S \frac{\partial s}{\partial t} \, . \tag{3-9}$$

During the transformation processes, not only the aquifer is transformed from an

anisotropic one into an isotropic one, but also the relative position of stream against

pumping well is changed. Such a position change is illustrated as follows.

Firstly, in the $\alpha\beta$ system, intercepts on α and β axis are $(a,0)$ and $(0, -b)$ which can be

calculated as

$$a = \frac{X_0}{cos\theta} \; ; \; b = \frac{X_0}{sin\theta} \; . \tag{3-10}$$

Secondly, in the α^*, β^* system, which is shown in Figure 3. Stream intercepts the α^*

and β^* axes at $\left(a^{'},0\right)$ and $\left(0,-b^{'}\right)$, respectively, and the intercepts satisfy

$$a^{'} = a\sqrt{\frac{T_\beta}{T_e}}; \quad b^{'} = b\sqrt{\frac{T_\alpha}{T_e}} \; . \tag{3-11}$$

Thirdly, in the $\alpha^* \beta^*$ system, in order to derive drawdown equation, an image recharge

well is added on the other side of the stream, which is symmetric with the real pumping

well against the stream and has the same magnitude as the pumping rate. Perpendicular

distance between the pumping well and stream (denoted as l in Figure 3) equals to

$$l = \frac{\left|a^{'} \; b^{'}\right|}{\sqrt{a^{'2}+b^{'2}}} = \frac{\sqrt{T_e}|ab|}{\sqrt{T_\beta a^2 + T_\alpha b^2}} \; . \tag{3-12}$$

Therefore, based on the property of symmetry, the coordinate of the image recharge well

in the $\alpha^* \beta^*$ system is $(\frac{2l^2}{a^{'}}, -\frac{2l^2}{b^{'}})$
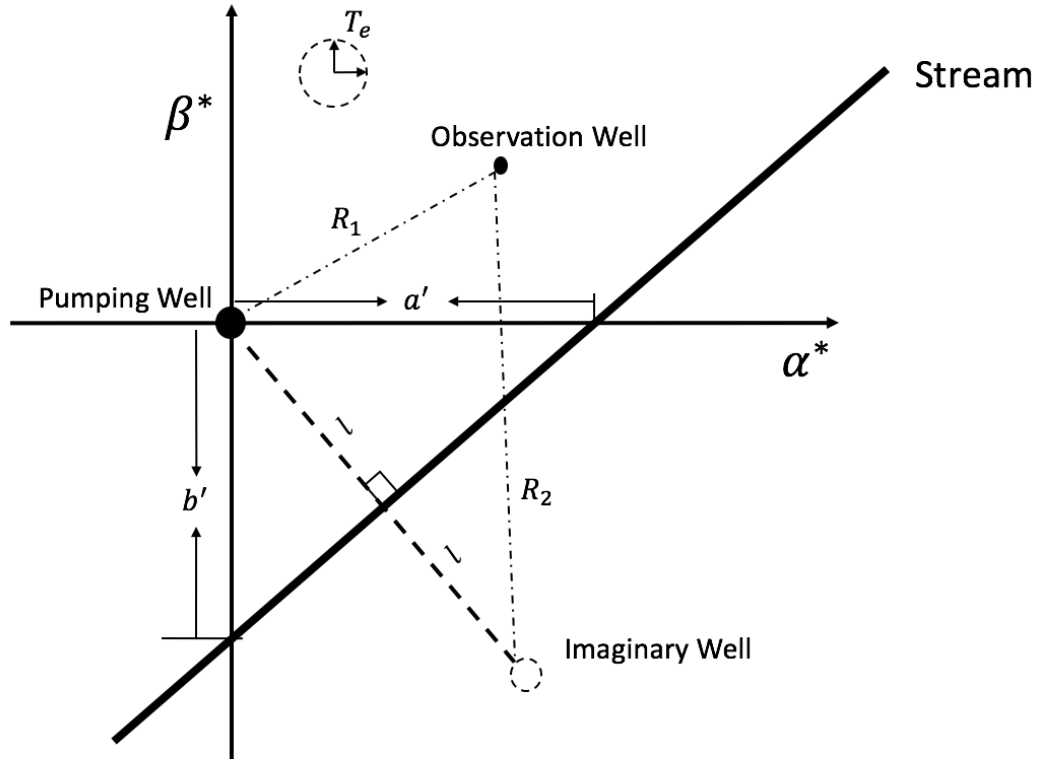
Figure 3: The study area is shown in the $\alpha^*\beta^*$ coordinate system.

The location of the observation well in the *XY* coordinate system is (X_1, Y_1). After the coordinate transformation procedures as outlined above, the location of the observation well in the $\alpha^* \beta^*$ coordinate system is (α_1^*, β_1^*). The drawdown at this observation well is a summation of drawdown caused by the pumping well and buildup induced by the image recharge well,

$$s = \frac{Q}{4\pi T_e}\left[W\left(u_{R_1}\right) - W(u_{R_2})\right] , \qquad (3\text{-}13)$$

$$W\left(u_{R_1}\right) = \int_{\frac{R_1{}^2 S}{4T_e t}}^{\infty} \frac{e^{-\lambda}}{\lambda} d\lambda; \quad W\left(u_{R_2}\right) = \int_{\frac{R_2{}^2 S}{4T_e t}}^{\infty} \frac{e^{-\lambda}}{\lambda} d\lambda ; \qquad (3\text{-}14)$$

$$R_1{}^2 = (\alpha_1^*)^2 + (\beta_1^*)^2; \tag{3-15}$$

$$R_2{}^2 = (\alpha_1^* - \frac{2l^2}{a'})^2 + (\beta_1^* - \frac{2l^2}{-b'})^2 = R_1{}^{2^2} + 4l^2\left(1 - \frac{\alpha_1^*}{a'} + \frac{\beta_1^*}{b'}\right), \tag{3-16}$$

where R_1 and R_2 are the distances between the observation well and the real pumping well

and the image recharge well, respectively.

To obtain the drawdown equation in the XY system, Eq. (3-13) should be transformed

back into the $\alpha\beta$ system first. The relationship of coordinates of the observation well in

the α β systems satisfies

$$\alpha_1^* = \sqrt{\frac{T_\beta}{T_e}}\alpha_1; \quad \beta_1^* = \sqrt{\frac{T_\alpha}{T_e}}\beta_1. \tag{3-17}$$

Consequently, Eq. (3-15) and Eq. (3-16) can be respectively transformed into

$$R_1{}^2 = \frac{T_\beta\alpha_1{}^2 + T_\alpha\beta_1{}^2}{T_e}; \tag{3-18}$$

$$R_2{}^2 = R_1{}^2 + 4l^2\left(1 - \frac{\alpha_1}{a} + \frac{\beta_1}{b}\right). \tag{3-19}$$

Fourthly, the relationship of coordinates of the observation well in the $\alpha\beta$ and XY

systems satisfies

$$\begin{cases} \alpha_1 = X_1\cos\theta + Y_1\sin\theta \\ \beta_1 = -X_1\sin\theta + Y_1\cos\theta \end{cases}. \tag{3-20}$$

Therefore, Eq. (3-18) can be expressed using the XY coordinates considering Eq. (3-6)

and Eq. (3-20), and it becomes (see Appendix A)

$$R_1{}^2 = \frac{T_{XX}Y_1^2 + T_{YY}X_1^2 - 2T_{XY}X_1Y_1}{T_e}. \tag{3-21}$$

Additionally, from Eq. (3-6), the expressions of T_α and T_β are also derived, and the

detailed procedures are listed in Appendix A

$$T_\alpha = \frac{cos^2\theta T_{XX} - sin^2\theta T_{YY}}{cos^2\theta - sin^2\theta} \; ; \tag{3-22}$$

$$T_\beta = \frac{cos^2\theta T_{YY} - sin^2\theta T_{XX}}{cos^2\theta - sin^2\theta} \; ; \tag{3-23}$$

$$a^2 T_\beta + b^2 T_\alpha = T_{XX}(a^2 + b^2) \; . \tag{3-24}$$

By substituting Eqs. (3-21) to (3-24), Eq. (3-19) can also be transformed into the XY system (see Appendix A)

$$R_2{}^2 = R_1{}^2 + \frac{4T_e ab}{T_{XX}(a^2+b^2)} [ab - X_1(bcos\theta + asin\theta) + Y_1(acos\theta - bsin\theta)] \; . \tag{3-25}$$

Substituting Eqs. (3-8), (3-10), (3-21) and (3-26) into Eq. (3-13), the drawdown equation in the XY system is

$$\begin{cases} s = \frac{Q}{4\pi T_e}\left[W(u_{R_1}) - W(u_{R_2})\right] = \frac{Q}{4\pi T_e}\left(\int_{u_{R_1}}^{\infty} \frac{e^{-\lambda}}{\lambda} d\lambda - \int_{u_{R_2}}^{\infty} \frac{e^{-\lambda}}{\lambda} d\lambda\right) \\ \quad u_{R_1} = \frac{R_1^2 S}{4T_e t}; \quad u_{R_2} = \frac{R_2^2 S}{4T_e t}; \\ \quad T_e = \sqrt{T_{XX}T_{YY} - T_{XY}^2} \; ; \end{cases} \tag{3-26}$$

Eq. (3-26) will serve as the working equation for the following analysis.

3.2 Data Interpretation

With above preparation, one is able to conduct the pumping test data interpretation for a horizontally anisotropic aquifer. I start with the interpretation in a confined aquifer first. After that, interpretation in an unconfined aquifer will follow on the basis of the confined aquifer interpretation. Kruseman et al. (1994) and Batu (1998) summarized a library of methods of analyzing various pumping test data in details. Unfortunately, none of those methods concern the pumping test near a stream in a horizontally anisotropic aquifer. The

procedures that will be discussed in the following will fill a knowledge gap not covered in the books mentioned before.

In a horizontally anisotropic aquifer with unknown principal directions, at least three observation wells are needed to determine the aquifer properties (Papadopulos, 1965; Hantush, 1966). Figure 4 shows the positon of three observation wells and a pumping well. r_1, r_2 and r_3 are the radial distances between the pumping well and three observation wells, respectively. As defined previously, the α and β axes are the principal transmissivity directions, and the α axis makes η angle with r_1. And, r_1 makes ξ and γ angle with r_2 and r_3, separately. Consequently, the α axis makes angle $\eta+\xi$ and $\eta+\gamma$ with r_2 and r_3, respectively. A positive η means that r_1 is on the counter-clockwise side of the α axis. Conversely, a negative η means that r_1 is on the clockwise side of the α axis.
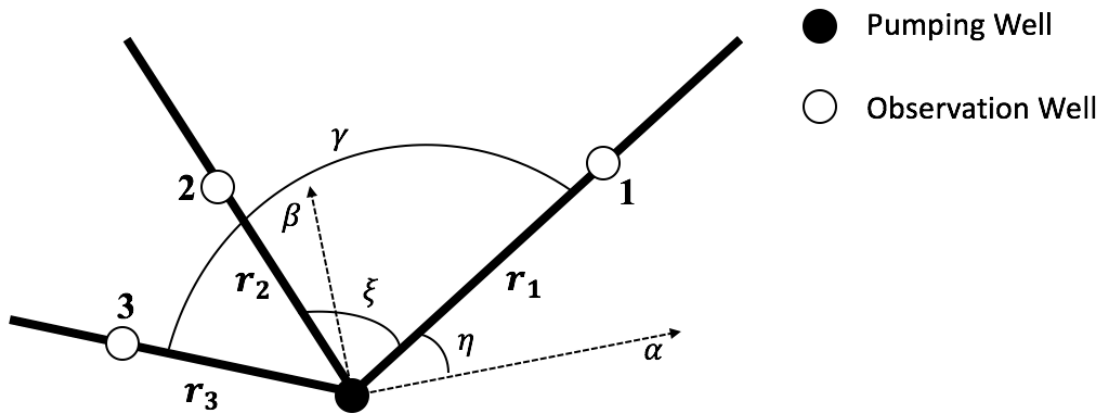

Figure 4: The position of pumping well and three non-collinear observation wells.

Based on observed drawdowns in three observation wells, the pumping test interpretation is illustrated step by step as follows. Because the analytical steps are exactly the same for data from three observation wells, the first observation well is chosen as an example to explain the interpretation procedures.

Step 1: According to Eq. (3-26) derived in Chapter 3.1, one can define a new parameter $\varepsilon = \frac{R_2}{R_1}$. Meanwhile, based on the series form of Theis well function (Batu, 1998), Eq. (2-1) can be transformed into

$$s = \frac{Q}{4\pi T} W(u) = \frac{Q}{4\pi T}\left(-0.5772 - \ln u - \sum_{n=1}^{\infty}(-1)^n \frac{u^n}{n \cdot n!}\right). \tag{3-27}$$

Similarly, Eq. (3-26) can be rewritten as

$$s = \frac{Q}{4\pi T_e}\left[W(u_{R_1}) - W(\varepsilon^2 u_{R_1})\right] = \frac{Q}{4\pi T_e}\left[2\ln(\varepsilon) + \sum_{n=1}^{\infty}(-1)^n(\varepsilon^{2n} - 1)\frac{u_{R_1}^n}{n \cdot n!}\right]. \tag{3-28}$$

When pumping time is large enough, which satisfies $(\varepsilon^2 u_{R_1}) \leq 0.01$, Eq. (3-28) can be approximated as (Hantush, 1959)

$$s = \frac{Q}{4\pi T_e}\left[2\ln(\varepsilon) - (\varepsilon^2 - 1)\frac{(\frac{R_1^2 S}{4T_e})}{t} + (\varepsilon^4 - 1)\frac{(\frac{R_1^2 S}{4T_e})^2}{2 \cdot 2! \cdot t^2}\right]. \tag{3-29}$$

Above equations work for a confined aquifer. It is notable that Eq. (3-29) is a quadratic function of $1/t$. However, problems involving stream depletion often occur in unconfined aquifers. In the following, a straightforward modification of the procedures for a confined aquifer is provided to be applicable for an unconfined aquifer. Actually, if the pumped aquifer is unconfined and the water table variation is much smaller than the saturated (pre-pumping) thickness of the unconfined aquifer (less than 10%), one may simplify the

18

nonlinear flow equation in the unconfined aquifer into a linear equation with an adjusted

($s^{'}$) based on the observed drawdown (s) as follows (Batu, 1998)

$$s^{'} = s - \frac{s^2}{2d},\qquad\qquad(3\text{-}30)$$

where d is the initial saturated thickness of unconfined aquifer. After such a transformation, one can adopt the same procedures for a confined aquifer to interpret the adjusted $s^{'}$. In all the following discussion, I will use the same symbol s for both confined and unconfined measured drawdowns, and if it is for an unconfined aquifer, it actually means the $s^{'}$ term in Eq. (3-30).

If, however, the drawdown in the unconfined aquifer cannot be regarded as much smaller than the initial saturated thickness of the unconfined aquifer (greater than 10%), then the nonlinearity of the unconfined flow probably becomes significant enough to render the analytical interpretative procedure invalid (Hantush, 1964). For such circumstances, one needs to call in a numerical method to interpret the pumping test data, which is out of the scope of this thesis, but will be explored in a future study.
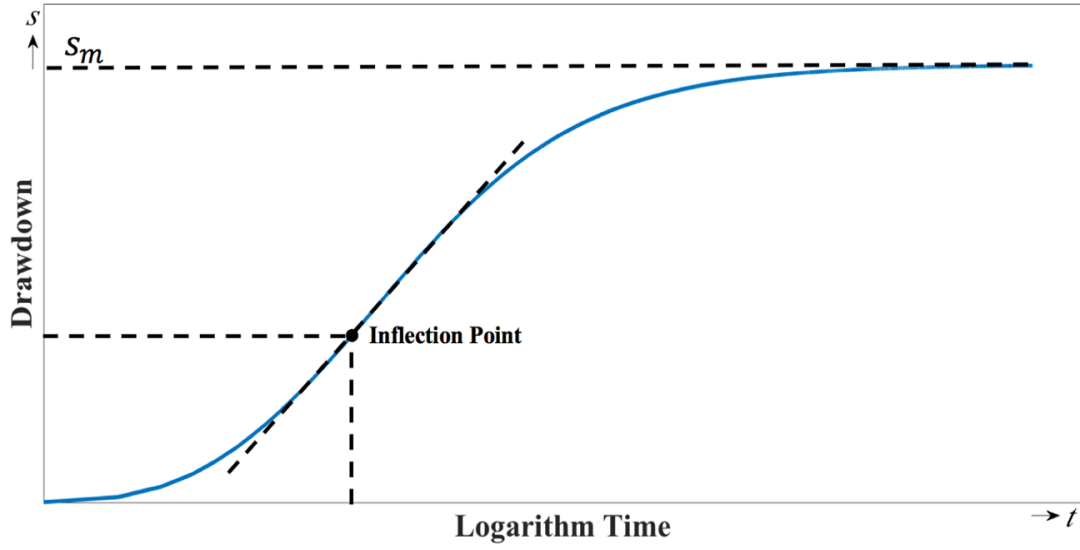
Figure 5: Drawdown in an observation well versus logarithm time (After Kruseman et al., 1994).

Step 2: According to observed drawdown data during the pumping test, plot the drawdown versus logarithm of time. As shown in Figure 5, there is an inflection point on the drawdown-time curve, at which the second derivative of Eq. (3-29) with respect to $ln(t)$ equals to zero. At such an inflection point, the value of u_{R_1} satisfies (Kruseman et al., 1994)

$$u_{R_1} = \frac{2ln(\varepsilon)}{\varepsilon^2 - 1} .$$ (3-31)

Putting Eq. (3-31) into the first derivative of Eq. (3-29) with respect to $log(t)$, the result is the geometric slope (m_1) at the inflection point (Kruseman et al., 1994) as

$$m_1 = \frac{2.303Q}{4\pi T_e} \left(e^{-u_{R_1}} - e^{-\varepsilon^2 u_{R_1}} \right) .$$ (3-32)

In addition, the maximum drawdown s_m is also related with ε as (Hantush, 1959)

$$s_m = \frac{Q}{2\pi T_e} ln(\varepsilon) .$$ (3-33)

Step 3: Drawdown data can also be used to plot the drawdown versus reciprocal time (1/*t*), as shown in Figure 6. This curve intercepts the vertical axis at the maximum drawdown s_m in Figure 6, and the geometric slope at such an intercept is $-m_t$, which satisfies (Batu, 1998)

$$m_t = \frac{Q}{4\pi T_e}(\varepsilon^2 - 1)\frac{R_1{}^2 S}{4T_e}. \tag{3-34}$$
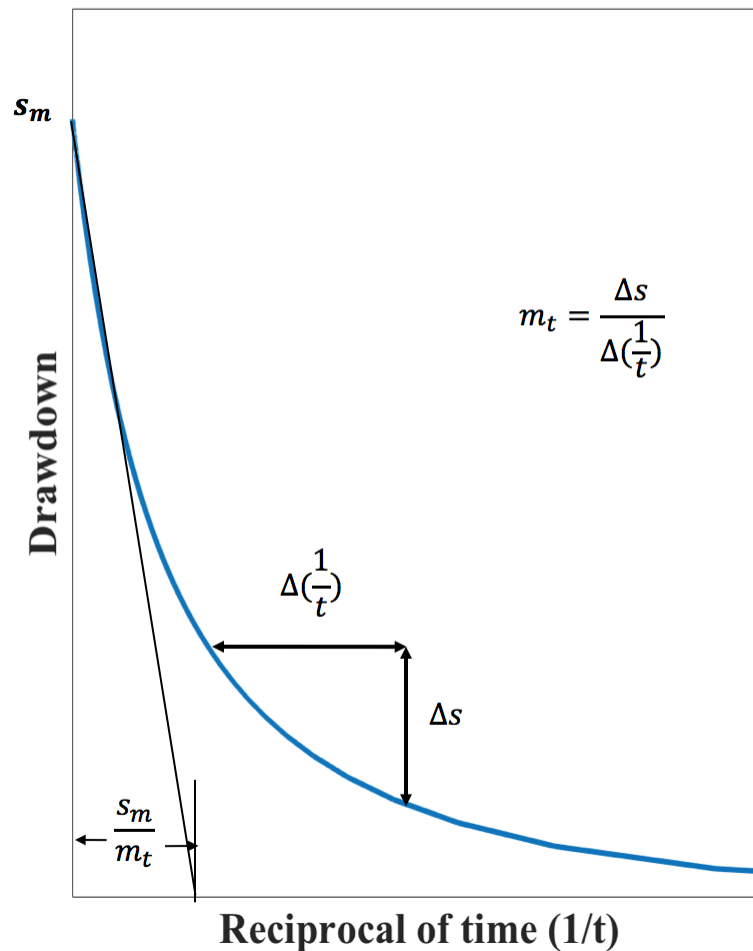

Figure 6: Drawdown in observation well versus (1/*t*) (Batu, 1998)

Substituting Eq. (3-33) and Eq. (3-34) into Eq. (3-29) leads to

$$s = s_m - \frac{m_t}{t} + \frac{c}{t^2} \; ; \qquad (3\text{-}35)$$

$$c = \frac{Q}{4\pi T_e}(\varepsilon^4 - 1)\frac{R_1{}^4 S^2}{64 T_e{}^2} \; . \qquad (3\text{-}36)$$

It is worthwhile to see that Eq. (3-35) is a quadratic function in respect to $1/t$ (similar to above Eq. (3-29)) with three coefficients of s_m, $-m_t$, and c.

Before determining values of aquifer parameters, the exact location of the inflection point cannot be determined. Therefore, the geometric slope at the inflection point is always approximated by the slope of a straight portion of the curve shown in Figure 5, which can be measured directly (Batu, 1998).

To facilitate the data analysis, one can employ a statistical software, like Statistical Analysis System (SAS), to do the following tasks: 1) Importing drawdown-time data into the software to plot drawdown versus logarithm time like Figure 4; 2) Determining the straight-line portion from the obtained curve; 3) The SAS software will establish a best-fitted linear equation for such a straight-line portion, and yield m_1, which can be considered as the slope of the inflection point.

Using the same way in respect to the analysis of Figure 5 to get the drawdown-$1/t$ curve as shown in Figure 6, and find a best-fitted quadratic equation (see Eq. (3-35)). Corresponding coefficients of such a quadratic equation are the values of s_m, $-m_t$ and c, respectively. Consequently, the ratio of s_m/m_1 is a known constant. Simultaneously, according to Eqs. (3-32) and (3-33),

$$\frac{s_m}{m_1} = \frac{2\log(\varepsilon)}{e^{-u_{R_1}} - e^{-\varepsilon^2 u_{R_1}}} \; . \qquad (3\text{-}37)$$

The left side of Eq. (3-37) is now a known constant and the right side of Eq. (3-37) is only related with ε, so the value of ε can be calculated directly.

Because the values of ε and s_m are both known based on above processes, substituting them into Eq. (3-33), T_e is solved straightforward. Three T_e values can be obtained by analyzing drawdown data from three observation wells, using the same procedures outlined above, and such three T_e values should be close to each other. A mathematical mean of such three T_e values may be regarded as the best estimation of its actual value. Besides that, substituting the obtained ε into Eq. (3-31), the value of u_{R_1} at the inflection point is calculated, which can be substituted together with ε into Eq. (3-29) to determine the drawdown at the inflection point (s_i). Based on the calculated s_i, one can locates the inflection point on the drawdown-time curve shown in Figure 5, and gets the corresponding time (t_i).

Step 4: In a horizontally anisotropic aquifer, one has

$$u_{R_1} = \frac{R_1^2 S}{4 T_e t} = \frac{r_1^{\,2} S}{4 T_{r_1} t} . \qquad (3\text{-}38)$$

where $r_1^{\,2} = X_1^2 + Y_1^2$ and (X_1, Y_1) are the coordinates of the first observation well. And T_{r_1} is the corresponding radial transmissivity in the r_1 direction. In the field, once the location of the observation well is determined, the value of r_1 can be measured directly. In regard to the inflection point, the corresponding values of t_i and u_{R_1} have been obtained in Step 3. Therefore, based on Eq. (3-38), hydraulic diffusivity in the r_1 direction $D_1 = \frac{T_{r_1}}{S}$ can be calculated using the following equation

$$D_1 = \frac{r_1^2}{4u_{R_1}t_i}. \tag{3-39}$$

Conducting the same processes for other two observation wells, one can get values of D_2 and D_3

$$D_2 = \frac{T_{r_2}}{S}; \quad D_3 = \frac{T_{r_3}}{S}, \tag{3-40}$$

where T_{r_2} and T_{r_3} are the radial transmissivity values in the directions of the second and the third observation wells, respectively. From above definitions of hydraulic diffusivity, it is obvious that

$$\frac{T_{r_1}}{T_{r_2}} = \frac{D_1}{D_2}; \quad \frac{T_{r_1}}{T_{r_3}} = \frac{D_1}{D_3}. \tag{3-41}$$

In a horizontally anisotropic aquifer, the relation between the radial transmissivity and the principal transmissivity is (Batu, 1998)

$$\begin{cases} T_{r_1} = \dfrac{T_\alpha}{cos^2\eta + \frac{T_\alpha}{T_\beta}sin^2\eta} \\ T_{r_2} = \dfrac{T_\alpha}{cos^2(\eta+\xi) + \frac{T_\alpha}{T_\beta}sin^2(\eta+\xi)} \\ T_{r_3} = \dfrac{T_\alpha}{cos^2(\eta+\gamma) + \frac{T_\alpha}{T_\beta}sin^2(\eta+\gamma)} \end{cases} \tag{3-42}$$

Step 5: In the field, the values of ξ and γ can be measured directly. Because of the unknown principal anisotropy direction, η is also unknown, but it can be calculated using the following equation (Batu, 1998)

$$tan(2\eta) = -2\frac{\left(\frac{D_1}{D_3}-1\right)sin^2\xi - \left(\frac{D_1}{D_2}-1\right)sin^2\gamma}{\left(\frac{D_1}{D_3}-1\right)sin(2\xi) - \left(\frac{D_1}{D_2}-1\right)sin(2\gamma)}. \tag{3-43}$$

All items on the right side of Eq. (3-43) are known, thus η can be solved straightforwardly. Considering the properties of tangent function involved in Eq. (3-43), there should be two

values of η, which deviate by $90°$. The following step will decide which one is the true solution and which one is false. In this regard, one can define a new parameter p as follows

$$p = \frac{T_\alpha}{T_\beta} = (\frac{T_e}{T_\beta})^2 \, . \tag{3-44}$$

After knowing values of three angles, p can be calculated using Eq. (3-45) (Batu, 1998)

$$p = \frac{cos^2(\eta+\xi)-\frac{D_1}{D_2}cos^2\eta}{\frac{D_1}{D_2}sin^2\eta-sin^2(\eta+\xi)} \, . \tag{3-45}$$

As defined in Chapter 2.1, $T_\alpha > T_\beta$, which will lead to $p > 1$. Therefore, the values of η which leads to $p < 1$ will be rejected, and the one results in $p > 1$ is accepted.

The angle between r_1 and the X axis plus the calculated value of η is the degree of θ, the angle between the T_α and X axes. Finally, based on the solved p, T_e and Eq. (3-44), T_α and T_β can be found out. One can then use Eq. (3-42) to get the corresponding radial transmissivity. After that, according to the definition of hydraulic diffusivity, the aquifer storativity, which also means specific yield of unconfined aquifer can be determined straightforwardly.

3.3 Stream Depletion

After getting the aquifer parameter values, the subsequent steps are used to calculate stream depletion. A fundamental formula for calculating stream depletion is the differential drawdown equation in an isotropic and infinite aquifer (Glover and Balmer, 1954)

$$ds = \frac{Q}{4\pi Tt} e^{\frac{-r^2 S}{4Tt}} dt, \tag{3-46}$$

where *ds* and *dt* are infinitesimally small increment of drawdown and time. For an horizontally anisotropic infinite aquifer, one can modify above Eq. (3-46) based on Eq. (3-26) to have

$$ds = \frac{Q}{4\pi T_e t} e^{-\left(\frac{T_{XX}Y^2 + T_{YY}X^2 - 2T_{XY}XY}{T_e}\right)S} \Bigg/ 4T_e t \, dt .$$
(3-47)

Darcy's law introduces that

$$q = \bar{\bar{T}} \cdot J .$$
(3-48)

where q is the discharge vector per unit width, $\bar{\bar{T}}$ is the transmissivity tensor, and J is the hydraulic gradient. Based on Eq. (3-47), one has

$$\begin{cases} J_X = \frac{ds}{dX} = \int_0^t \frac{Q}{4\pi T_e t} \cdot e^{\frac{-(T_{XX}Y^2 + T_{YY}X^2 - 2T_{XY}XY)S}{4T_e^2 t}} \cdot \frac{(2T_{XY}Y - 2T_{YY}X)S}{4T_e t} dt \\ J_Y = \frac{ds}{dY} = \int_0^t \frac{Q}{4\pi T_e t} \cdot e^{\frac{-(T_{XX}Y^2 + T_{YY}X^2 - 2T_{XY}XY)S}{4T_e^2 t}} \cdot \frac{(2T_{XY}X - 2T_{XX}Y)S}{4T_e t} dt \end{cases} .$$
(3-49)

For a horizontally anisotropic aquifer, Eq. (3-2) is substituted into Eq. (3-48),

$$\begin{vmatrix} q_X \\ q_Y \end{vmatrix} = \begin{vmatrix} T_{XX} & T_{XY} \\ T_{YX} & T_{YY} \end{vmatrix} \cdot \begin{vmatrix} J_X \\ J_Y \end{vmatrix} = \begin{vmatrix} T_{XX}J_X + T_{XY}J_Y \\ T_{YX}J_X + T_{YY}J_Y \end{vmatrix} .$$
(3-50)

The component of water flux that perpendicular to Y axis at $X=X_0$ equals to

$$q_{X=X_0} = T_{XX} \cdot J_X|_{X=X_0} + T_{XY} \cdot J_Y|_{X=X_0} .$$
(3-51)

When the principal transmissivities are known, T_{XX} and T_{XY} can be solved through Eq. (3-6).

Above discussion is for a laterally infinite aquifer without the stream. If, however, there is a stream with a constant stage fully penetrating the aquifer at $X=X_0$ without any hydraulic barrier separating the stream from the aquifer, such a stream can be treated as a CHB which supplies addition flow to the pumped aquifer. Thus, total water flux through

$X=X_0$ can be divided into two components: the first part is induced by the pumping well, which comes from aquifer storage; the second part is provided by the stream. These two parts have the same quantity and direction. Therefore, the total water flux equals to the double of q_X calculated in above Eq. (3-51). The total stream depletion rate over the entire stream during a given time (t) should be the integral of Eq. (3-51) with respect to L

$$Q_D = \int_{-\infty}^{+\infty} 2 \cdot q_{X=X_0} dL .$$
(3-52)

where L means the stream length.

3.4 Influence of Anisotropy

T_α/T_β represents the extent of anisotropy, a larger ratio means a greater anisotropy. The value of θ determines the direction of principal transmissivity. Based on Chapters 3.1 and 3.2, it is obvious to find that both T_α/T_β and θ control the characteristics of horizontal anisotropy. One can use the following procedures to inspect the influence of T_α/T_β and θ. Firstly, one can compare the difference of stream depletion rate under different values of T_α/T_β such as 4:1, 25:1, 50:1. Secondly, one can compute the stream depletion rate for θ values varying from 0 to $\frac{\pi}{2}$. Based on the symmetry of geometry, when θ varies in other quadrants, the stream depletion rate variation is similar to that when θ varies in the first quadrant.

I will use the following example to demonstrate the application of the new solutions of calculating the drawdowns and stream depletion rates and new pumping test data interpretation procedures proposed above.

4. EXAMPLE

Hantush (1959) conducted a 7-day pumping test in Norbert Irsik site near the Arkansan River, in the Ingalls area, Kansas. The pumped aquifer is unconfined, which is composed of alluvial deposits, and the saturated aquifer thickness before pumping is about 6.7 m. Pumping well with a rate of $0.044 \text{ m}^3/\text{s}$ is 41.15 m from the Arkansas River, and fully penetrates the aquifer. Arkansas River fully penetrates the aquifer as well. The distribution of observation wells is shown in Figure 7. The coordinates of three observation wells are (-8.5m, 10.5 m), (0, -19.8 m) and (17.4 m, 0), respectively. Hantush (1959) assumed the aquifer as horizontally isotropic, and the obtained transmissivity and storativity of the aquifer are $0.0228 \text{ m}^2/\text{s}$ and 0.11 from his analysis, respectively. A minor point to note is that the transmissivity for an unconfined aquifer is approximated by a product of hydraulic conductivity and the saturated thickness and vertical flow is neglected in this analysis.

In the following, we will generate a hypothetical case based on the work of Hantush (1959) by assuming the aquifer to be horizontally anisotropic rather than isotropic with the major principal direction forming an angle of $60°$ from the *X* axis (see Figure 7).
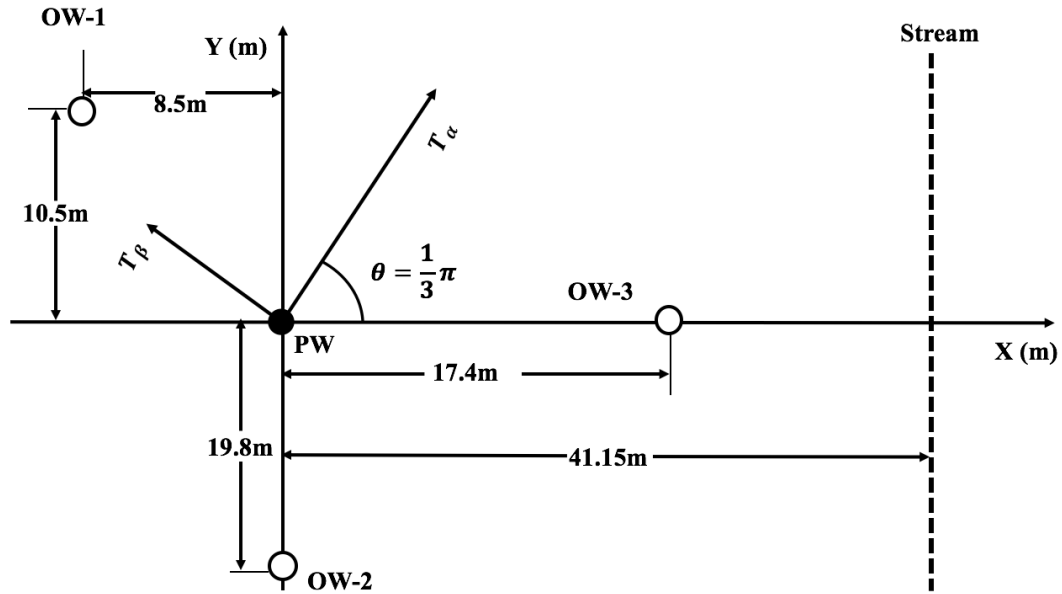
Figure 7: The map of studied area and locations of pumping well and observation wells.

4.1 Drawdown Curve

This section is devoted to compute the drawdowns and analyze the drawdown-time curves. Firstly, the isotropic case studied in Hantush (1959) can be considered as a special condition of horizontal anisotropy, which satisfies that $T_\alpha = T_\beta = T_e = 0.0228 \text{ m}^2/\text{s}$. To reflect the difference of drawdown between horizontally isotropic and anisotropic conditions, the values of T_e under these two scenarios should keep constant and one only changes the ratio of T_α/T_β in the following analysis. Without losing generality, $\frac{T_\alpha}{T_\beta} = 4$ is used as an example for the anisotropic condition. Nevertheless, one has $T_\alpha = 0.0456 \text{ m}^2/\text{s}$ and $T_\beta = 0.0114 \text{ m}^2/\text{s}$. Other values of $\frac{T_\alpha}{T_\beta}$ can be used as well if needed.

Secondly, because the drawdown calculation processes are exactly the same for three observation wells, OW-1 is chosen as an example in the following. In Eq. (3-26), the information used for calculating R_1 and R_2 includes: the coordinates of observation well in the XY system, the intercepts of stream on the α and β axes, which are denoted as $(a, 0)$ and $(0. -b)$, respectively, and the transmissivity components in the XY system. Based on Eqs. (3-6), (3-10), one has

$$a = \frac{41.15}{cos\frac{1}{3}\pi} = 82.28 \text{ m} \qquad b = \frac{41.15}{sin\frac{1}{3}\pi} = 47.51 \text{ m}. \qquad (4\text{-}1)$$

$$T_{XX} = 0.02 \text{ m}^2/\text{s}; \ \ T_{YY} = 0.037 \text{ m}^2/\text{s}; \ \ T_{XY} = 0.015 \text{ m}^2/\text{s} \ . \qquad (4\text{-}2)$$

Then, substituting Eqs. (4-1), (4-2) into Eqs. (3-21), (3-25), $R_1{}^2$ and $R_2{}^2$ are found to be 329.8 m^2 and 9.67×10^3 m^2, respectively. Finally, substituting the value of $R_1{}^2$ and $R_2{}^2$ into Eq. (3-26), drawdown can be calculated. Using the same procedures to deal with other two observation wells OW-2 and OW-3, one can get drawdowns for all three observation wells and the results are listed in Appendix B. The drawdown-time curves of three observation wells for a horizontally anisotropic case in semi-logarithmic scales are shown in Figure 8. For the purpose of comparison, drawdowns in three observation wells under equivalent isotropic condition are also computed and shown in Figure 8.
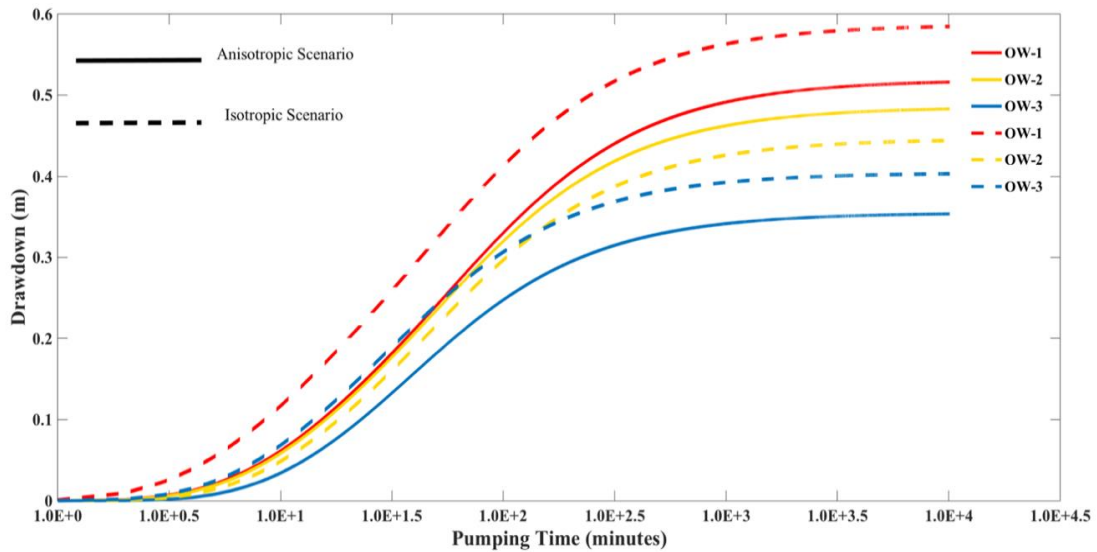
Figure 8: Drawdown in three observation wells under two different scenarios.

One can see from Figure 8 that the overall drawdown-time curves for an anisotropic case follow somewhat similar S-shapes as those for an isotropic case, but drawdowns for an anisotropic case can deviate significantly from their counterparts for an isotropic case at a given time. Furthermore, drawdowns for an anisotropic case can be greater or less than their counterparts at a given time depending on the location of the observation well. Figure 8 indicates that if one adopts a horizontally isotropic curve to interpret pumping test data of a horizontally anisotropic aquifer, considerable errors can be generated. Figure 8 signifies the importance of acknowledge the horizontal anisotropy for pumping test data interpretation.

31

4.2 Aquifer Parameters

This section is devoted to the pumping test interpretation. Basically, I will use the

procedures outlined in Chapter 3.2 to interpret the drawdowns calculated in Chapter 4.1

to see if I can reproduce the two principal transmissivities, storativity, and the angle of the

major principal transmissivity from the X axis.

According to the geometric relationship among observation wells as shown in Figure

7, the angles between r_1 and r_2 (ξ), r_1 and r_3 (γ) are $\frac{7}{9}\pi$ and $\frac{23}{18}\pi$, respectively, and the

angle between r_1 and X axis is $\frac{13}{18}\pi$. The radial distances between observation wells and

pumping well are 13.5 m, 19.8 m and 17.4 m, respectively.

A prerequisite of having quadratic relationship between drawdown and reciprocal

pumping time is $u_{R_2} \leq 0.01$ (as shown in Eq. (3-35)). The alluvium in the Ingalls area

primarily consists of stream-laid deposits that range from clayed silt to very coarse gravel.

Gravels compose the bulk of the alluvium, and are predominantly fine to medium and

poorly sorted (Stramel et al., 1958). Domenico and Schwartz (1998) listed that the

hydraulic conductivity of gravels ranges from 3×10^{-4} m/s to 3×10^{-2} m/s. Thus, the

assumed average hydraulic conductivity of the studied domain is 3×10^{-3} m/s. Because

the saturated thickness of the aquifer before pumping is 6.7 m, the transmissivity is about

0.02 m^2/s. Additionally, the specific yield in an unconfined aquifer usually ranges from

0.1 to 0.3 (Lohman, 1972). Therefore, the average specific yield of pumped aquifer is set

as 0.2. According to these assumptions, for OW-1, when the pumping time is more than

25 minutes, $u_{R_2} \leq 0.01$ is satisfied. Thus, I import the drawdown data after 25 minutes into SAS to find the best-fitted quadratic equation as follows,

$$s = 0.52 - 1.39 \times 10^3 \times \frac{1}{t} + 1.45 \times 10^6 \times \frac{1}{t^2}. \tag{4-3}$$

Based on the coefficients in Eq. (3-35), s_m equals to 0.52.

Now, I use entire drawdown data to plot a drawdown versus logarithm time curve, and determine the straight portion of the curve. After this step, the straight portion data is imported into SAS to identify its slope, which has

$$m_1 = 0.28 . \tag{4-4}$$

After getting the values of s_m and m_1, the other related parameters can all be calculated using the following steps and the results are listed in Table 1. To facilitate the interpretation, I develop necessary MATLAB script files listed in Appendix C.

Firstly, based on Eq. (3-37), $\frac{s_m}{m_1} = 1.85$. Using the MATLAB program to find ε=6.2.

Secondly, based on Eq. (3-31), u_{R_1} and u_{R_2} are found to be 0.1 and 3.75, respectively.

Thirdly, substituting the calculated u_{R_1} and u_{R_2} into Eq. (3-28), the drawdown and time values at the inflection point are found. Finally, based on Eqs. (3-33) and (3-39), T_e and D are determined. The above procedures used for observation well OW-1 can be directly applied to other two observation wells OW-2 and OW-3, and the related results are also listed in Table 1.

Table 1: Calculated results for three observation wells

	s_m (m)	m_1	$f(\varepsilon)$	ε	u_{R_1}	u_{R_2}	s_i (m)	t_i (min)	T_e (m²/s)	D (m²/s)
OW-1	0.52	0.28	1.85	6.2	0.10	3.75	0.26	58	0.025	0.13
OW-2	0.48	0.28	1.74	5.4	0.12	3.50	0.24	52	0.025	0.26
OW-3	0.35	0.23	1.48	3.8	0.20	2.87	0.16	41	0.027	0.15
Average									0.026	

Combining the obtained hydraulic diffusivity (D) with Eq. (3-43), the degree of angle η is solved. For OW-1, $\eta = -\frac{19}{180}\pi$ or $\eta = \frac{71}{180}\pi$. Substituting the values of η and ξ into Eq. (3-45), the value of p is then calculated. As defined previously, p should be greater than 1 for an anisotropic aquifer. While, when $\eta = -\frac{19}{180}\pi$, $p = 0.27$, which is less than 1 and should be rejected. Thus, the correct value of η is $\frac{71}{180}\pi$, and the corresponding p value is 3.75. Therefore, the value of θ can be calculated as

$$\theta = \frac{13}{18}\pi - \frac{71}{180}\pi = 59° .$$
(4-5)

Substituting the p value of 3.75 into Eq. (3-44), the principal transmissivities T_α and T_β are found,

$$T_\alpha = 0.050 \text{ m}^2/\text{s}; \quad T_\beta = 0.013 \text{ m}^2/\text{s}.$$
(4-6)

Combining Eq. (4-6) with Eqs. (3-40) and (3-42), the storativity (specific yield for the unconfined aquifer) equals to 0.1. Table 2 summaries the discrepancy between interpreted

and actual parameters. One can see the discrepancy is the least for θ (1.6%) and the greatest for T_β (14%), which are both below 15%. This implies that the proposed interpretative procedures in Chapter 3.2 are valid in explaining pumping data from horizontally anisotropic aquifer laterally bounded by a stream.

Table 2: Comparison of analyzed transmissivity, storativity and θ with theoretical value.

	T_α (m^2/s)	T_β (m^2/s)	S	θ (°)
Analyzed	0.050	0.013	0.1	59
Theoretical	0.0456	0.0114	0.11	60
Error Percentage	9.6%	14%	9.1%	1.6%

4.3 Depletion Comparison

In order to investigate the effect of horizontal anisotropy on stream depletion, one can change the values of T_α/T_β and θ individually to check their influences on stream depletion. It is notable that T_e remains constant when T_α/T_β varies. For instance, when T_e remains to be 0.0228 m^2/s, one has $\frac{T_\alpha}{T_\beta} = 25$, and $\frac{T_\alpha}{T_\beta} = 50$.
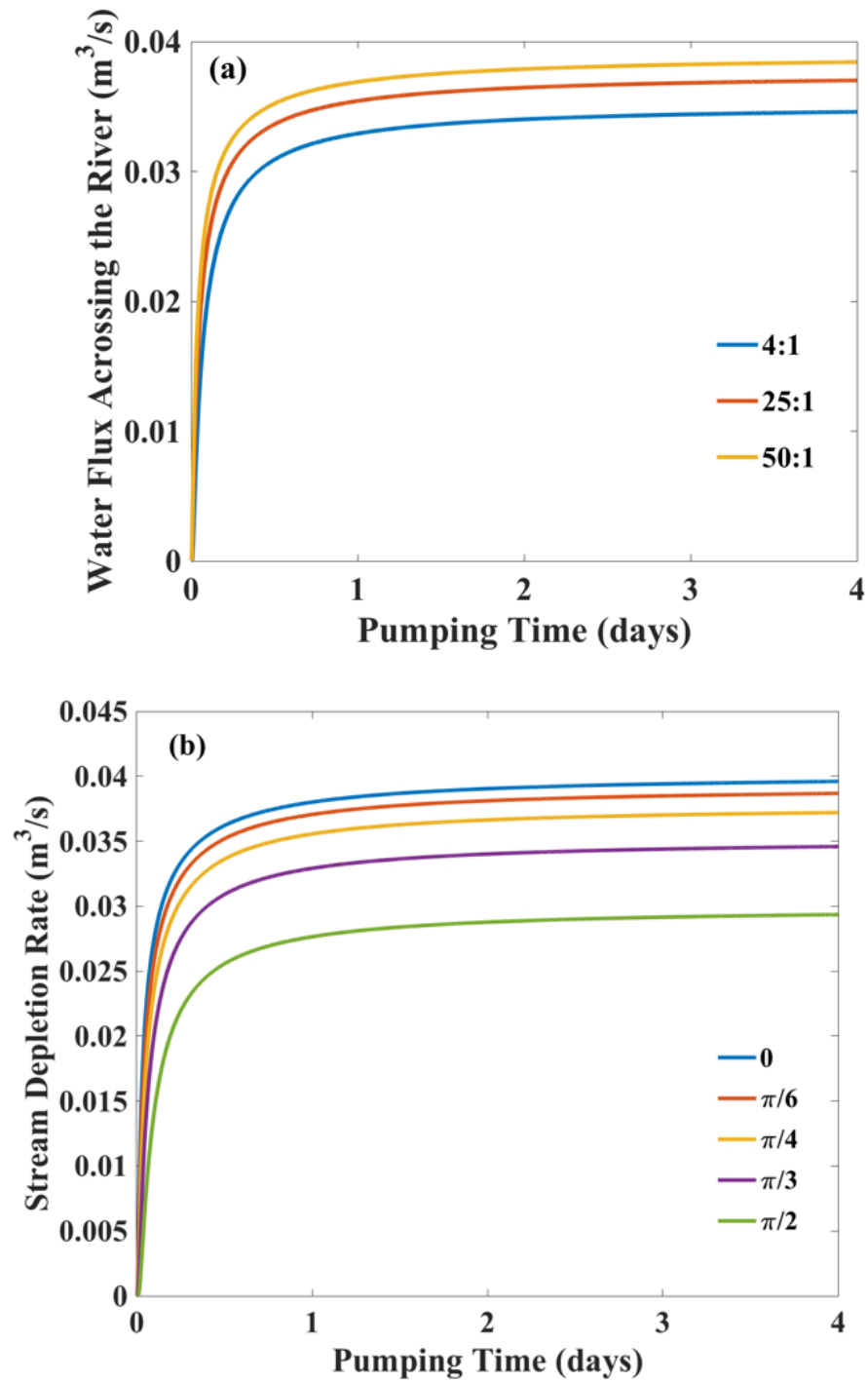
Figure 9: Stream depletion rate over the entire stream reach under different values of (a) T_α/T_β; (b) θ.

From Figure 9(a), it is obvious to see that a greater horizontal anisotropy will lead to a higher stream depletion rate. When T_α/T_β equals to 50, the depletion rate under steady state is about 0.039 m³/s, which represents 89% of the pumping rate which is 0.044 m³/s. While this depletion rate is just 0.035 m³/s for $\frac{T_\alpha}{T_\beta} = 4$, which is about 79% of the pumping rate. Although the difference of depletion rate among three scenarios does not appear to be significant in Figure 9(a), the difference of total depletion volume during the whole pumping period could be sizable. For example, after stream depletion reaches steady state, the total depletion volumes during a following 7-day pumping period for $\frac{T_\alpha}{T_\beta} = 50$ and $\frac{T_\alpha}{T_\beta} = 4$ are 2.36×10^4 m³ and 2.11×10^4 m³, respectively, with a difference of 2.5×10^3 m³. From United States Environmental Protection Agency (EPA), the average American family of four uses 2.6 m³ of water per day. Thus, aforementioned depletion volume difference could supply 32 families for one months. Therefore, one can conclude that horizontal anisotropy has significant impact on stream depletion amount, which will affect streamflow, aquatic ecosystem and the benefits of different stakeholders. As shown in Figure 9(b), when θ varies from 0 to $\frac{\pi}{2}$, the depletion rate decreases considerably.

5. FUTURE WORK

In this thesis, the derived drawdown equations and related interpretation procedures are based on a series of idealistic assumptions. These assumptions can be relaxed in some cases to accommodate the actual field conditions. Several future studies can be carried out on the basis of this thesis with the purpose of expanding the current knowledge base on investigating horizontally anisotropic aquifers:

1. Considering stream width: Zlotnik et al. (1999) derived an analytical model about stream depletion with a finite stream width in an isotropic aquifer. Future work with horizontally anisotropic media can be extended to accommodate this factor, probably on the basis of Zlotnik et al. (1999).

2. Partially penetrating stream: In the Great Plains, streams almost partially penetrate the surrounding aquifers (Zlotnik and Huang, 1999). The application of previous derived equations to a partially penetrating stream will result in the overestimation of stream depletion rate (Chen and Yin, 2004). Therefore, a future work could consider this factor.

3. Hydraulically disconnected: Field tests conducted along the Arkansas River in the southeastern Colorado reflected that pumping can easily lower the groundwater table below the streambed, which will break the hydraulic connection between the stream and the groundwater, and subsequent pumping may not greatly impact the stream depletion rate (Moore and Jenkins, 1966).

Developing appropriate analytical model for this condition in a horizontally anisotropic aquifer will be meaningful.

4. Semi-permeable barrier between the stream and aquifer: For some streams, there is a semi-permeable barrier separating the stream from the aquifer. For this case, the stream cannot be treated as a CHB. Instead, it can be treated as a GHB (Hantush, 1965). It will be interesting to extend the work of this thesis to this scenario.

Besides the aforementioned works, changing constant pumping rate into a time-dependent rate, such as harmonic pumping rate; considering nonlinear flow in the unconfined aquifer, and concerning the heterogeneity property of the aquifer can all serve as potential topics of investigation based on this thesis.

6. CONCLUSION

In this thesis, I investigate drawdown-time behavior caused by a pumping well near a stream in a horizontally anisotropic aquifer. I also investigate the stream depletion rate at a specific location of the stream and total stream depletion rate over the entire stream reach induced by the pumping well. This thesis shows that the drawdown and stream depletion equations for a horizontally anisotropic aquifer can be substantially different from their counterparts in a horizontally isotropic aquifer.

Because of the complexity of different transmissivity tensor involved in a horizontally anisotropic aquifer, i.e., the major and minor components of the principal transmissivities and the principal directions unknown, the pumping test interpretation procedures for a horizontally isotropic aquifer is substantially more complex than the standard interpretation procedures for a horizontally isotropic aquifer. I report a detailed and innovative procedure for interpreting the pumping test data for a horizontally isotropic aquifer in this thesis. It appears that minimum three non-collinear observation wells are needed for such a task. I also develop MATLAB script files to facilitate the computation of drawdown and stream depletion and then to aid the pumping test interpretation.

Based on results of this thesis, I conclude that the direction of principal transmissivity and anisotropic ratio considerably impact the drawdown and stream depletion rate for a horizontally anisotropic aquifer laterally bounded by a stream.

Some of the assumptions involved in this thesis can be relaxed to account for a variety of realistic field situations, and the related future researches are summarized in the final chapter.

REFERENCES

Barlow, P.M. and Leake, S.A., 2012. Streamflow depletion by wells: Understanding and managing the effects of groundwater pumping on streamflow. U.S. Geological Survey Circular 1376. Reston, Virginia: USGS.

Batu, V., 1998. Aquifer Hydraulics: A Comprehensive Guide to Hydrogeologic Data Analysis. Wiley, New York.

Bear, J., 1972. Dynamics of Fluids in Porous Media. American Elsevier Pub. Co., New York.

Butler, J.J., Zlotnik, V.A. and Tsou, M.S., 2001. Drawdown and stream depletion produced by pumping in the vicinity of a partially penetrating stream. Ground Water, 39(5), pp.651-659.

Butler, J.J., Zhan, X. and Zlotnik, V.A., 2007. Pumping-induced drawdown and stream depletion in a leaky aquifer system. Ground Water, 45(2), pp.178-186.

Chapuis, R.P., 1994. Assessment of methods and conditions to locate boundaries: I. one or two straight impervious boundaries. Ground Water, 32(4), pp.576-582.

Chen, X. and Yin, Y., 1999. Evaluation of streamflow depletion for vertical anisotropic aquifers. Journal of Environmental Systems, 27(1), pp.55-70.

Chen, X., 2000. Measurement of streambed hydraulic conductivity and its anisotropy. Environmental Geology, 39(12), pp.1317-1324.

Chen, X. and Chen, X., 2003. Effects of aquifer anisotropy on the migration of infiltrated stream water to a pumping well. Journal of Hydrologic Engineering, 8(5), pp.287-293.

Chen, X. and Yin, Y., 2004. Semianalytical solutions for stream depletion in partially penetrating streams. Ground Water, 42(1), pp.92-96.

Chen, X., 2007. Hydrologic connections of a stream–aquifer-vegetation zone in south-central Platte River valley, Nebraska. Journal of Hydrology, 333(2), pp.554-568.

Cheng, C., Song, J., Chen, X. and Wang, D., 2011. Statistical distribution of streambed vertical hydraulic conductivity along the Platte River, Nebraska. Water Resources Management, 25(1), pp.265-285.

Cihan, A., Zhou, Q., Birkholzer, J.T. and Kraemer, S.R., 2014. Flow in horizontally anisotropic multilayered aquifer systems with leaky wells and aquitards. Water Resources Research, 50(1), pp.741-747.

Cook, R. and Barlas, N., 2014. Aquifer anisotropy in the Pen Argyl Member of the Martinsburg formation, Pennsylvania. Environmental & Engineering Geoscience, 20(3), pp.273-285.

Domenico, P.A. and Schwartz, F.W., 1998. Physical and Chemical Hydrogeology, 2nd ed. John Wiley & Sons Inc, New York.

Ferris, J.G., Knowles, D.B., Brown, R.H. and Stallman, R.W., 1962. Theory of Aquifer Tests. US Geological Survey, Water-Supply Pap. 1536-E.

Foglia, L., McNally, A. and Harter, T., 2013. Coupling a spatiotemporally distributed soil water budget with stream-depletion functions to inform stakeholder-driven

management of groundwater-dependent ecosystems. Water Resources Research, 49(11), pp.7292-7310.

Glover, R.E. and Balmer, G.G., 1954. River depletion resulting from pumping a well near a river. Eos, Transactions American Geophysical Union, 35(3), pp.468-470.

Hantush, M.S. 1959. Analysis of data from pumping wells near a river. Journal of Geophysical Research, 65(5), pp.16727-1629.

Hantush, M.S., 1964. Drawdown around wells of variable discharge. Journal of Geophysical Research, 69(20), pp.4221-4235.

Hantush, M.S., 1965. Wells near streams with semipervious beds. Journal of Geophysical Research, 70(12), pp.2829-2838.

Hantush, M.S., 1966. Analysis of data from pumping tests in anisotropic aquifers. Journal of Geophysical Research, 71(2), pp.421-426.

Herschy, R.W. and Fairbridge, R.W. eds., 1998. Encyclopedia of Hydrology and Water Resources. Springer Science & Business Media, The Netherlands.

Hill, A.R., 1990. Ground water flow paths in relation to nitrogen chemistry in the near-stream zone. Hydrobiologia, 206(1), pp.39-52.

Hunt, B., 1999. Unsteady stream depletion from ground water pumping. Ground Water, 37(1), pp.98-102.

Hunt, B., 2009. Stream depletion in a two-layer leaky aquifer system. Journal of Hydrologic Engineering, 14(9), pp.895-903.

Jenkins, C.T., 1968. Techniques for computing rate and volume of stream depletion by wells. Ground Water, 6(2), pp.37-46.

Kalbus, E., Reinstorf, F. and Schirmer, M., 2006. Measuring methods for groundwater? surface water interactions: a review. Hydrology and Earth System Sciences Discussions, 10(6), pp.873-887.

Kruseman, G.P., De Ridder, N.A. and Verweij, J.M., 1994. Analysis and Evaluation of Pumping Test Data. International Institute for Land Reclamation and Improvement, The Netherlands.

Lebbe, L. and De Breuck, W., 1997. Analysis of a pumping test in an anisotropic aquifer by use of an inverse numerical model. Hydrogeology Journal, 5(3), pp.44-59.

Lohman, S.W., 1972. Ground-water Hydraulics. US Geological Survey, Professional Paper 708.

Mathias, S.A. and Butler, A.P., 2007. Flow to a finite diameter well in a horizontally anisotropic aquifer with wellbore storage. Water Resources Research, 43(7), W07501.

Moore, J.E. and Jenkins, C.T., 1966. An evaluation of the effect of groundwater pumpage on the infiltration rate of a semipervious streambed. Water Resources Research, 2(4), pp.691-696.

Neuman, S.P., Walter, G.R., Bentley, H.W., Ward, J.J. and Gonzalez, D.D., 1984. Determination of horizontal aquifer anisotropy with three wells. Ground Water, 22(1), pp.66-72.

Papadopulos, I.S., 1965. Nonsteady flow to a well in an infinite anisotropic aquifer. Proceedings of the Dubrovnik Symposium on the Hydrology of Fractured Rocks, International Association of Scientific Hydrology, Publication No. 73, pp.21-31.

Quiñones-Aponte, V., 1989. Horizontal anisotropy of the principal ground-water flow zone in the Salinas alluvial fan, Puerto Rico. Ground Water, 27(4), pp.491-500.

Sageev, A., Horne, R.N. and Ramey, H.J., 1985. Detection of linear boundaries by drawdown tests: A semilog type curve matching approach. Water Resources Research, 21(3), pp.305-310.

Singh, S.K., 2002. Aquifer boundaries and parameter identification simplified. Journal of Hydraulic Engineering, 128(8), pp.774-780.

Sophocleous, M., Townsend, M.A., Vogler, L.D., McClain, T.J., Marks, E.T. and Coble, G.R., 1988. Experimental studies in stream-aquifer interaction along the Arkansas River in central Kansas-Field testing and analysis. Journal of Hydrology, 98(3), pp.249-273.

Sophocleous, M., Koussis, A., Martin, J.L. and Perkins, S.P., 1995. Evaluation of simplified stream-aquifer depletion models for water rights administration. Ground Water, 33(4), pp.579-588.

Sophocleous, M., 2002. Interactions between groundwater and surface water: the state of the science. Hydrogeology Journal, 10(1), pp.52-67.

Stoner, J.D., 1981. Horizontal anisotropy determined by pumping in Two Powder river basin coal aquifers, Montana. Ground Water, 19(1), pp.34-40.

Stramel, G.J. Lane, C.W., Hodson, W.G., 1958. Geology and Ground-water Hydrology of the Ingalls Area, Kansas. University of Kansas Publications, State Geological Survey of Kansas Bulletin 132.

Theis, C.V., 1941. The effect of a well on the flow of a nearby stream. Eos, Transactions American Geophysical Union, 22(3), pp.734-738.

Tsou, P.R., Feng, Z.Y., Yeh, H.D. and Huang, C.S., 2010. Stream depletion rate with horizontal or slanted wells in confined aquifers near a stream. Hydrology and Earth System Sciences, 14(8), pp.1477-1485.

Yeh, H.D., Chang, Y.C. and Zlotnik, V.A., 2008. Stream depletion rate and volume from groundwater pumping in wedge-shape aquifers. Journal of Hydrology, 349(3), pp.501-511.

Wen, J.C., Wu, C.M., Yeh, T.C.J. and Tseng, C.M., 2010. Estimation of effective aquifer hydraulic properties from an aquifer test with multi-well observations (Taiwan). Hydrogeology Journal, 18(5), pp.1143-1155.

Winter, T.C., 1998. Ground Water and Surface Water: A Single Resource. US Geological Survey Circular 1139. US Geological Survey, Denver, Colorado.

Zlotnik, V.A. and Huang, H., 1999. Effect of shallow penetration and streambed sediments on aquifer response to stream stage fluctuations (analytical model). Ground Water, 37(4), pp.599-605.

Zlotnik, V.A., Huang, H. and Butler, J.J., 1999. Evaluation of stream depletion considering finite stream width, shallow penetration, and properties of streambed sediments. In Proceedings of Water 99, Joint Congress, Brisbane, Australia, pp.221-226.

APPENDIX A

1. Calculation of T_e.

$$T_{XX}T_{YY} - T_{XY}^2 = (T_\alpha cos^2\theta + T_\beta sin^2\theta)(T_\alpha sin^2\theta + T_\beta cos^2\theta)$$

$$-(T_\alpha - T_\beta)^2 sin^2\theta cos^2\theta$$

$$= T_\alpha T_\beta(sin^4\theta + 2sin^2\theta cos^2\theta + cos^4\theta)$$

$$= T_\alpha T_\beta(sin^2\theta + cos^2\theta)^2$$

$$= T_\alpha T_\beta \,. \tag{A-1}$$

2. Calculation of R_1^2

$$R_1^2 = T_\beta(X_1 cos\theta + Y_1 sin\theta)^2 + T_\alpha(-X_1 sin\theta + Y_1 cos\theta)^2$$

$$= X_1^2(T_\alpha sin^2\theta + T_\beta cos^2\theta) + Y_1^2(T_\alpha cos^2\theta + T_\beta sin^2\theta) -$$

$$2X_1 Y_1 sin\theta cos\theta(T_\alpha - T_\beta)$$

$$= T_{YY}X_1^2 + T_{XX}Y_1^2 - 2T_{XY}X_1 Y_1 \,. \tag{A-2}$$

3. Calculation of T_α and T_β

The steps about calculating T_α and T_β are the same. So, the steps T_β is not

repeated. Based on Eq. (3-7),

$$\begin{cases} cos^2\theta T_{XX} = T_\alpha cos^4\theta + T_\beta sin^2\theta cos^2\theta \\ sin^2\theta T_{YY} = T_\alpha sin^4\theta + T_\beta sin^2\theta cos^2\theta \end{cases}$$

$$\Longrightarrow cos^2\theta T_{XX} - sin^2\theta T_{YY} = T_\alpha(cos^4\theta - sin^4\theta) = T_\alpha(cos^2\theta - sin^2\theta)$$

$$\Longrightarrow T_\alpha = \frac{cos^2\theta T_{XX} - sin^2\theta T_{YY}}{cos^2\theta - sin^2\theta} \,. \tag{A-3}$$

4. Calculation of $a^2 T_\beta + b^2 T_\alpha$

Based on Eq. (3-11), $\sin\theta = \dfrac{m}{b}$ and $\cos\theta = \dfrac{m}{a}$

$$a^2 T_\beta + b^2 T_\alpha = \frac{a^2(\cos^2\theta T_{YY} - \sin^2\theta T_{XX}) + b^2(\cos^2\theta T_{XX} - \sin^2\theta T_{YY})}{\cos^2\theta - \sin^2\theta}$$

$$= \frac{a^2\left(\dfrac{m^2}{a^2}T_{YY} - \dfrac{m^2}{b^2}T_{XX}\right) + b^2\left(\dfrac{m^2}{a^2}T_{XX} - \dfrac{m^2}{b^2}T_{YY}\right)}{\dfrac{m^2}{a^2} - \dfrac{m^2}{b^2}}$$

$$= T_{XX}\frac{b^4 - a^4}{b^2 - a^2}$$

$$= T_{XX}(a^2 + b^2). \tag{A-4}$$

5. Calculate $R_2{}^2$

$$R_2{}^2 = (R_1)^2 + 4\left(\frac{\sqrt{T_\alpha T_\beta}|ab|}{\sqrt{a^2 T_\beta + b^2 T_\alpha}}\right)^2\left(1 - \frac{\sqrt{T_\beta}\alpha_1}{a\sqrt{T_\beta}} + \frac{\sqrt{T_\alpha}\beta_1}{b\sqrt{T_\alpha}}\right)$$

$$= R_1{}^2 + \frac{4T_e^2 ab}{T_{XX}(a^2 + b^2)}(ab - b\alpha_1 + a\beta_1)$$

$$= R_1{}^2 + \frac{4T_e^2 ab}{T_{XX}(a^2+b^2)}[ab - b(X_1\cos\theta + Y_1\sin\theta) + a(-X_1\sin\theta +$$

$$Y_1\cos\theta)] \tag{A-5}$$

$$= R_1{}^2 + \frac{4T_e^2 ab}{T_{XX}(a^2+b^2)}[ab - X_1(b\cos\theta + a\sin\theta) + Y_1(a\cos\theta - b\sin\theta)].$$

APPENDIX B

Table 3: Simulated drawdown data for three observation wells.

Time （minutes）	s_{OW-1} (m)	s_{OW-2} (m)	s_{OW-3} (m)
0	0	0	0
1	2.70E-05	1.99E-05	7.20E-07
2	0.0013	0.0011	0.0002
5	0.0200	0.0184	0.0077
10	0.0616	0.0585	0.0343
15	0.0978	0.0939	0.0620
25	0.1534	0.1487	0.1084
40	0.2116	0.2062	0.1578
60	0.2647	0.2578	0.2004
120	0.3516	0.3396	0.2619
180	0.3944	0.3784	0.2886
240	0.4199	0.4009	0.3034
300	0.4367	0.4156	0.3128
360	0.4487	0.4260	0.3193
540	0.4700	0.4442	0.3306
840	0.4864	0.4582	0.3390
1140	0.4946	0.4650	0.3430
1440	0.4995	0.4691	0.3454
1800	0.5032	0.4723	0.3473
2160	0.5058	0.4744	0.3485
2520	0.5076	0.4759	0.3494
2880	0.5090	0.4771	0.3501
3240	0.5100	0.4780	0.3506
3600	0.5109	0.4787	0.3510
3960	0.5116	0.4793	0.3514
4320	0.5122	0.4798	0.3517
4680	0.5127	0.4802	0.3519
5040	0.5131	0.4806	0.3521
5440	0.5135	0.4809	0.3523
5760	0.5138	0.4811	0.3525
6120	0.5141	0.4814	0.3526

6480	0.5144	0.4816	0.3527
6840	0.5146	0.4818	0.3528
7200	0.5148	0.4820	0.3529
7560	0.5150	0.4821	0.3530
7920	0.5152	0.4823	0.3531
8280	0.5153	0.4824	0.3532
8640	0.5155	0.4825	0.3533
9000	0.5156	0.4826	0.3533
9360	0.5157	0.4827	0.3534
9720	0.5158	0.4828	0.3534
10080	0.5159	0.4829	0.3535

APPENDIX C

1. MATLAB script for calculating drawdown in different observation wells.

```
X=-8.5; Y=10.5;    % the coordinate of observation well
Q=0.044;      %pumping rate
T1=0.0456;T2=0.0114;    % principal transmissivity
de=pi/3;       % the angle between T1 and X axis
T=604800;      % pumping time
m=41.15;       % perpendicular distance between stream and pumping well
S=0.11;       % storativity
Te=sqrt(T1*T2);
Se=S/Te;
a=m/cos(de);b=m/sin(de);
Txx=T1*(cos(de))^2+T2*(sin(de))^2;
Tyy=T2*(cos(de))^2+T1*(sin(de))^2;
Txy=(T1-T2)*cos(de)*sin(de);
R1=Txx*Y^2+Tyy*X^2-2*Txy*X*Y;
R2=R1+4*Te^2*a*b*(a*b-X*(b*cos(de)+a*sin(de))+Y*(a*cos(de)-b*sin(de)))/(Txx*(a^2+b^2));
t=0:60:T;
s=zeros(length(t),1);
lgt=zeros(length(t),1);
for i=1:length(t)
   u1=R1*Se/(4*Te*t(i));
   u2=R2*Se/(4*Te*t(i));
   lgt(i)=log10(t(i)/60);
   w1=expint(u1);
   w2=expint(u2);
   s(i)=Q*(w1-w2)/(4*pi*Te);
end
```

2. MATLAB script for calculating ε

Because Eq. (3-37) is so complicated that the function like fzero and solve in Matlab cannot be used to calculate the value of ε for each observation well, trail and error method is adopted.

```
x=[5:0.1:15]; % x represents ε
sm=0.47;     % maximum drawdown derived from quadratic model
m1=0.27;  % the slope of straight portion of drawdown versus logarithmic time
ratio=sm/m1
c=zeros(length(x),1);
for i=1:length(x)
u=2*log(x(i))/(x(i)^2-1);
```

```
a=exp(-u);
b=exp(-u*x(i)^2);
d=2*log10(x(i))/(a-b);
c(i)=ratio-d;
end
```

3. MATLAB script for calculating stream depletion amount

```
clc, clear;
syms t y;

Q=-0.044;   % pumping rate
T1=0.0456;T2=0.0114;   % principal transmissivity
theta=pi/3;   % the angle between T1 and X axis
T=604800;   % pumping time
x=41.15;   % perpendicular distance between stream and pumping well
S=0.11;   % storativity
Te=sqrt(T1*T2);
Se=S/Te;
Txx=T1*(cos(theta))^2+T2*(sin(theta))^2;
Tyy=T2*(cos(theta))^2+T1*(sin(theta))^2;
Txy=(T1-T2)*cos(theta)*sin(theta);

F1=Q./(4*pi*Te.*t);
F2=(Se.*(-(Txx.*y.^2+Tyy*x^2-2*Txy*x.*y)))./(4*Te.*t);
F3=(Se*(2*Txy.*y-2*Tyy*x))./(4*Te.*t);
F4=(Se*(2*Txy*x-2*Txx.*y))./(4*Te.*t);

q1=Txx*F1.*F3.*exp(F2);
q2=Txy*F1.*F4.*exp(F2);
q=q1+q2;

fun = matlabFunction(q);

dt = 60;
Vmat = zeros(1,(T)/dt);
Vmat(1) = 2*integral2(fun,0,1,-150,150);

i = 2;
for tmax = (dt+1):dt:T
    Vmat(i) = Vmat(i-1)+2*integral2(fun,tmax-dt,tmax,-150,150);
    i = i+1;
end


plot(1:dt:T,Vmat);
xlabel('t')
legend('V')
```